

University of Victoria

Department of Physics & Astronomy

**Analysis of Contact Fabrication for**  
**CdZnTe X-ray Detectors**

By

Malcolm Newson

Redlen Technologies Inc.

Sidney, B.C.

## Introduction:

Redlen Technologies is a Saanich based company involved in the development and manufacturing of Cadmium Zinc Telluride (CZT) semiconductor x-ray detectors, which is one of the most promising materials for the next generation of solid detectors. Due to its high atomic number, suitable band-gap energy, and ability to function at room temperature, CdZnTe is suitable for many applications in the fields of medical imaging, process monitoring, and national security, where specifications set by those applications require that these detectors operate without significant cooling in extreme conditions while maintaining good resolution, high detector efficiency, good reliability, and high throughput.

The alternative detectors include Germanium or Silicon semiconductor detectors and scintillator detectors. The semiconductors all directly convert the incoming x-ray into electrons, measured as current, and constitute the signal. In contrast, the scintillator is a two-step conversion where the incident x-ray is converted into visible light and then into electrons. The major drawback of Germanium is that it requires cooling to liquid nitrogen temperatures, making it impossible to have as a portable detector.

Detectors consist of a CZT body and metal contacts on the anode and cathode sides that connect the body to the required electronics. The type of contact can have significant effects on the response characteristics of the detector. CZT detectors at Redlen must pass screenings that select which detectors continue to final fabrication stages and recycled or re-fabricated. This testing involves subjecting them to x-ray bombardment and measuring the response characteristics of individual pixel count rate and short term stability (Lag) and the detectors' total mean and standard deviation of both count rate and lag. Lag is a measure of how the pixel's count rate response changes over a short time frame, where a positive lag pixel will have a count rate that increases over time.

In Figure 1 four different detectors' lag results are shown. A) displays good mean ( $m=0.13$ ) and standard deviation ( $sd=0.65$ ) values, B) displays negative mean lag, C) displays a line feature that would disqualify the detector, and D) displays a spot feature that would also disqualify that detector.

## Background:

X-rays are high energy photons that can be detected through their interactions with materials like solid-state semiconductor devices. In this case, the incident photon transfers its energy into a valence shell electron, bumping it up into a conducting band and leaving a hole in the valence band. With a voltage bias maintained over the detector, the holes and electrons are attracted to their respective terminals and induce an electrical signal.

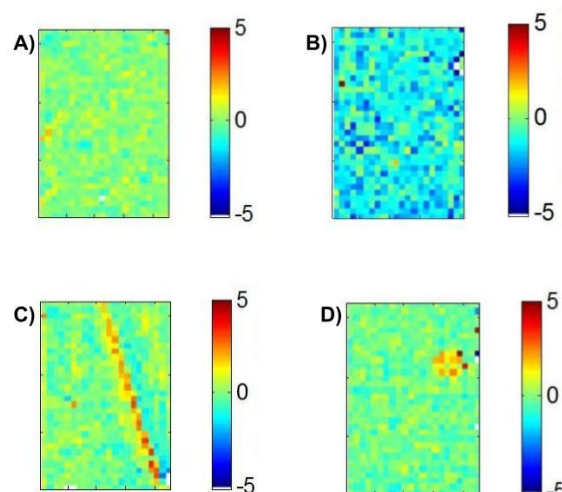


Figure 1: A) Good lag with  $m = 0.13$  and  $sd = 0.65$ . B) Bad negative lag at  $m = -1.30$ . C) Line defect. D) Spot defect.

Detectors are manufactured with pixels on the anode side that allow for positional detection of the x-ray to a smaller area than the total detector size. When tested, each pixel has its own count rate and lag. A good detector will have an average count rate, the standard deviation of count rate, average lag, and standard deviation of lag that are all within specifications. They will also need to lack distinct features such as spots or lines in the lag map. Taken together, these characteristics constitute stability on both the pixel scale and the detector scale.

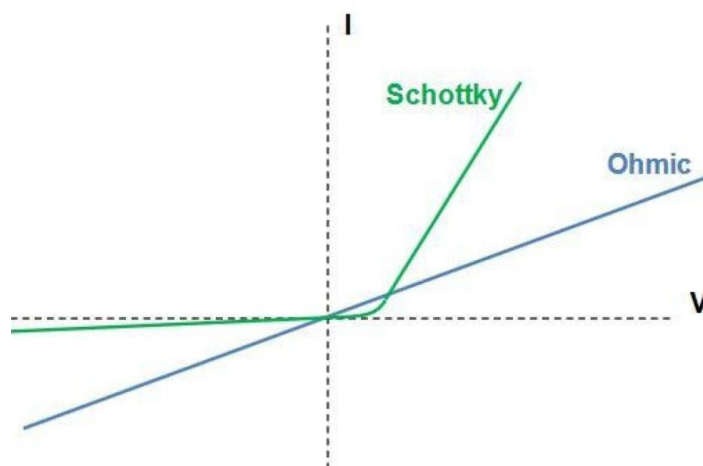


Figure 2: Ohmic and Schottky Detector I-V Characteristics

Two types of contacts are used: rectifying (Schottky) and non rectifying (Ohmic). A non-rectifying contact has a linear current response to both positive and negative voltage bias applied across the detectors and rectifying has a non-linear response.

Measurements of the current response to voltage will produce a plot similar to Figure 2 and are described by equation

$$I = AA^*T^2 \exp\left(\frac{-q\phi_B}{kT}\right) \left[ \exp\left(\frac{qV}{nkT}\right) - 1 \right]$$

where A is the effective device area,  $A^*$  is the Richardson's constant, T is the temperature in Kelvin, q is the charge of an electron, V is the applied voltage, n is the diode ideality factor, K is Boltzmann's constant, and  $\phi_B$  is the effective barrier height (eV).

On a semilog plot, there is a linear portion of the I-V curve at low voltage; this linear portion can be extrapolated to determine the y-intercept (defined as b) which is used to give the saturation current  $I_s = e^b$ . The effective barrier height is calculated using

$$\phi_B = \frac{KT}{q} \ln\left(\frac{AA^*T^2}{I_s}\right).$$

## Contact study:

To explore how both the metal used for the contact and different surface treatment processes affect the output of the detector, detectors with a good lag response, negative lag, and positive lag were selected for refabrication. The three surface treatment processes before metal deposition are As Polished (AP), BrMeOh (Br), and Plasma Passivation (PP). Gold (Au) is deposited using an electroless chemical solution, and Platinum (Pt) is deposited using Electron-beam physical vapor deposition. The E-beam technique has the sample in a vacuum chamber above the Platinum sample. An electron beam incident on the sample causes vaporized Platinum to rise and condense on the sample.

To refabricate a detector, the old metal contacts are polished off using a basic mechanical polishing lapper and a pre-prepared slurry of progressively smaller granule size. Next, one of the surface preparations is used to remove any oxidation, except in the As Polished case where metal is deposited without any surface treatment. In the BrMeOh group, a chemical etch of Bromine Methanol at 2% concentration is applied for about 1 minute to remove approximately 20 nm of the material.

For the plasma passivation, a vacuum chamber is separately purged with Argon and Oxygen gas. High voltage is applied between two plates on the top and bottom of the chamber, creating a strong electric field that will attract the gas's electrons and ions towards the respective plates. Hence the detector placed on the bottom of the chamber is bombarded with the ions. When Argon, a noble and relatively heavy gas, is purged, it collides with the surface atoms and removes a top layer and "cleans" the surface. On the next step, Oxygen is purged into the chamber where the ions upon collision with the surface help to cause an oxide layer to grow.

After surface preparation and metal deposition, the detectors need a single large pixel on the anode side. This is done using a chemical lithography process where a photoresist layer is applied using spin coating. The tile is exposed under a mask to UV light for 60 seconds, which causes a chemical change in the photoresist that allows areas not exposed to UV light to be dissolved using a developer. A final chemical etching removes the metal not protected by photoresist, and the pixel structure is created. Final polishing of the side walls removes any metal contact that might provide a direct conductive path around the crystal bulk. After chemical etching, the crystal is rinsed in a gradually diluted methanol solution followed by a final rinse in acetone, IPA (2 min each), and blown dry with pressurized nitrogen gas.

## Results:

Figures 3 & 4 below show an I-V curve's results for each tile for the voltage range of  $[-300, 300]$  at 300K with 40 sample points spaced linearly on the logarithmic voltage axis. All of the gold tiles are consistent with an Ohmic contact where the I-V response is symmetric. The platinum tiles display some odd behavior, but a subgroup shows an explicit Schottky contact behavior. Some show symmetric responses like the gold ohmic contacts. However, some others show very unusual behavior, possibly due to a lack of robustness for tile level platinum deposition. All of the Platinum results can be seen in Appendix A.

To calculate the Ideality factor, Saturation current, and the Barrier height using the equations described above, the tiles were retested for the voltage range  $[-2, 2]$  so that the low voltage linear response could be utilized with higher resolution. The

following are the results from good tiles that displayed the expected response for the range [-300, 300].

Pt - Plasma - Good	n = 9.8782
Pt - As Pol - Good	n = 11.71
Pt - Br - Good	n = 13.428
Au - Plasma - Good	n = 8.05
Au - As Pol - Good	n = 8.8462
Au - Br - Good	n = 8.8462

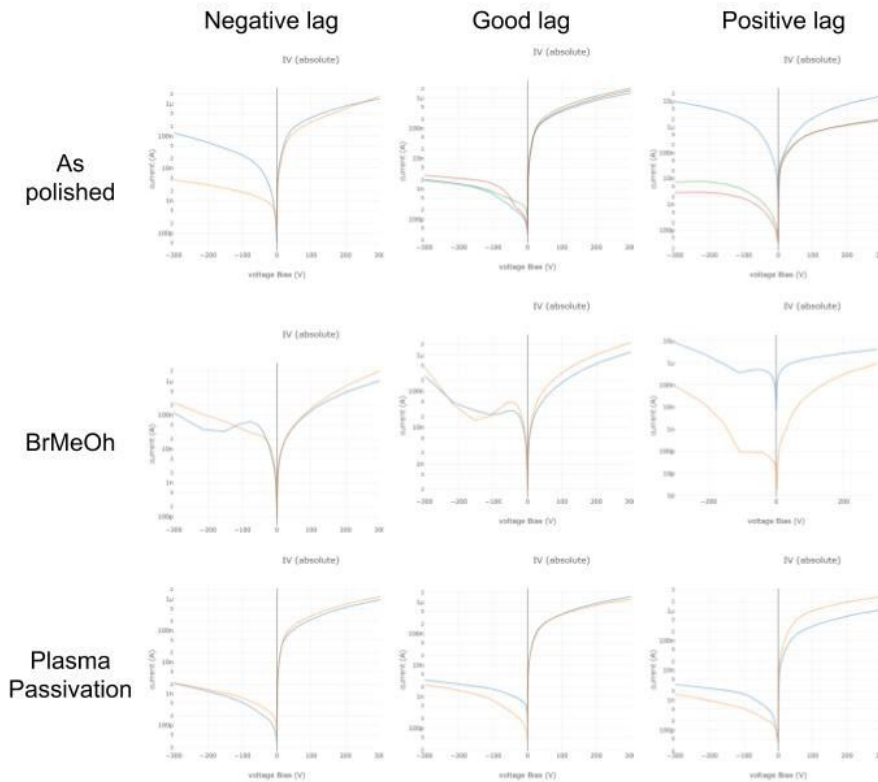
Patrick P Beck (2010, p. 36) states that the ideality factor should be close to  $n = 1$  for a perfect thermionic emission model, but will approach  $n = 2$  as contributions from generation-recombination current increases. As other current mechanisms become significant, the ideality factor can increase above 2. With values higher than  $n = 1.1$ , contributions from other sources are too significant to calculate the saturation current for a Thermionic Emissions model alone; thus, the barrier height calculated from saturation current will have no physical interpretation.

## Future Research:

The first and most obvious step to follow up this study is to increase the sample size and attempt to discover a production pattern that causes some of the unexpected behavior in Platinum samples. This may depend on improving the method of metal deposition in the Electron Beam process.

The process for Plasma Passivation, unfortunately, used a small amount of bromine. Ideally, some modifications to that process could remove the bromine use so that the Plasma Passivation group and BrMeOH group can be independent.

## Appendix A:



Appendix A: Platinum Tile Results

## References :

Beck, Patrick R. (2010). *Measurement and Modeling of Blocking Contacts for Cadmium Telluride Gamma Ray Detectors*. United States. doi:10.2172/990413.

Sadeghi, N. (2019). The Effect of Crystal Defects on the Performance of High-flux CZT X-ray Detectors. Retrieved 22 August 2019, from <http://dspace.library.uvic.ca/handle/1828/6754>

Sellin, P., Prekas, G., Franc, J., & Grill, R. (2010). Electric field distributions in CdZnTe due to reduced temperature and x-ray irradiation. *Applied Physics Letters*, 96(13), 133509. doi: 10.1063/1.3373526